

Unified Approach to Probing Coulomb Effects in Tunnel Ionization for Any Ellipticity of Laser Light

A. S. Landsman,^{*} C. Hofmann, A. N. Pfeiffer, C. Cirelli, and U. Keller
Physics Department, ETH Zurich, CH-8093 Zurich, Switzerland
(Received 20 August 2013; published 26 December 2013)

We present experimental data that show significant deviations from theoretical predictions for the location of the center of the electron momenta distribution at low values of ellipticity ϵ of laser light. We show that these deviations are caused by significant Coulomb focusing along the minor axis of polarization, something that is normally neglected in the analysis of electron dynamics, even in cases where the Coulomb correction is otherwise taken into account. By investigating ellipticity-resolved electron momenta distributions in the plane of polarization, we show that Coulomb focusing predominates at lower values of ellipticity of laser light, while Coulomb asymmetry becomes important at higher values, showing that these two complementary phenomena can be used to probe long-range Coulomb interaction at all polarizations of laser light. Our results suggest that both the breakdown of Coulomb focusing and the onset of Coulomb asymmetry are linked to the disappearance of Rydberg states with increasing ellipticity.

DOI: [10.1103/PhysRevLett.111.263001](https://doi.org/10.1103/PhysRevLett.111.263001)

PACS numbers: 32.80.Fb, 32.80.Ee, 32.80.Rm, 34.10.+x

Tunnel ionization is believed to underlie many important phenomena in ultrafast science, whereby the combined Coulomb-laser field creates a potential barrier through which an electron can tunnel out of the atom and be accelerated by the strong laser field [1–7]. Due to the presence of a strong infrared field, after ionization the electron experiences primarily the force of the laser, with the force of the parent ion assumed to exert only a weak perturbation. Historically, this perturbation has been neglected, in an approach known as the strong field approximation [8,9]. More recently, an approach has been proposed by Goreslavski *et al.* [10] that follows the classical trajectory of the electron after it appears at the tunnel exit, calculating the force of the parent ion as a perturbation along this trajectory. This approach predicts a Coulomb correction predominantly in the direction of tunneling, corresponding to the shift in the center of the electron momenta distribution largely along the major axis of polarization, and leading to asymmetry in electron momenta distributions [11].

It has therefore typically been assumed that the Coulomb correction along the minor axis of polarization is negligible [6,11,12]. This assumption has been used in reconstructing electron dynamics involved in high harmonic generation (HHG) [6,12], where small ellipticity [12] or a weak transverse 2nd harmonic [6] was used to probe the dynamics along the major axis of polarization. Using this framework, the perturbative dynamics were described by neglecting the Coulomb field, resulting in decoupling between the motion along the major and minor axes of polarization, respectively, and, therefore, allowing reconstruction of ionization and return times of the electron [6] without making any classical assumptions about its position in the tunneling direction. Here, however, we experimentally observe a significant Coulomb correction to the electron momentum

along the minor axis of polarization for laser ellipticities $\epsilon < 0.3$, which includes values of ϵ well above the threshold where HHG is suppressed. Our results suggest that the Coulomb force along the direction of the weaker field should be accounted for when investigating electrons involved in HHG or in general any phenomena where laser fields with a weak transverse component are used.

Recent work [11,13] has focused on the impact of the Coulomb interaction on electron momenta distributions, investigating Coulomb asymmetry [4,11] and Coulomb focusing [13]. Hence, in Ref. [11], it was found that the initial transverse velocity and the phase of the electric field at the time of ionization, unconventionally referred to as “tunneling time” by the authors (for the conventional definition see, for instance, Ref. [14]), were important to Coulomb asymmetry, while in Ref. [13] significant Coulomb focusing was found perpendicular to the plane of polarization by studying transverse momenta distributions. Prior work on Coulomb focusing, investigated its impact on rescattering electrons [15,16]. However, such electrons are difficult to identify experimentally, and, therefore, such investigations had to rely on classical simulations of electron trajectories [13,15,16].

Here we adopt a different approach, identifying two independent observables, namely, the location of the center of the electron momenta distribution along the major and minor axis of polarization, as an independent probe of Coulomb asymmetry and Coulomb focusing, respectively. Since this approach uses only the center of the electron momenta distribution, it is easily accessible experimentally and very robust to noise. Using this method, neither transverse momenta spreads nor different phases of ionization are needed to detect Coulomb asymmetry or Coulomb focusing. Our investigation of experimentally measured

ellipticity-resolved electron momenta in the plane of polarization unifies the two widely studied phenomena, showing how Coulomb focusing begins to break down at about the same value of ellipticity where Coulomb asymmetry becomes significant.

The electric field of a laser is given by

$$\vec{F}(t) = \frac{-F_0 f(t)}{\sqrt{\epsilon^2 + 1}} [\cos(\omega t)\hat{x} + \epsilon \sin(\omega t)\hat{y}], \quad (1)$$

where ω is the frequency of the laser, ϵ is the ellipticity, with \hat{x} and \hat{y} taken to be the major and minor axes of polarization, respectively, and $f(t)$ is the pulse envelope. The center of the electron momenta distribution that is measured at the detector is then given by $\vec{P} = P_x\hat{x} + P_y\hat{y}$ (see Fig. 1) and corresponds to ionization at the peak of the electric field, or along the x axis, with drift momentum subsequently acquired predominantly along the y axis. A standard technique in strong field ionization, following Simpleman's model [17–20], is to neglect the Coulomb field after ionization [6,12,21,22] and treat the dynamics classically, much as it is done in plasma physics [23–25]. In particular, if the Coulomb field along the minor axis of polarization is neglected, then the dynamics are determined solely by the y component of Eq. (1) [6], resulting in

$$P_y = \pm \frac{\epsilon F_0}{\omega\sqrt{\epsilon^2 + 1}} + P_{y0}, \quad (2)$$

where P_{y0} is the initial velocity at the tunnel exit [26,27], and the sign is determined by the direction of the electric field at the instance of ionization (0 or 180 deg). Figure 2 plots theoretical P_y (green curve), given by Eq. (2), taking $P_{y0} = 0$, in accordance with the most probable velocity predicted by the Ammosov-Delone-Krainov probability distribution at the tunnel exit [26].

Our experimental data, shown in Fig. 1 for low ($\epsilon = 0.2$) and high ($\epsilon = 0.7$) ellipticities, were obtained by recording electron momenta distributions in the plane of polarization

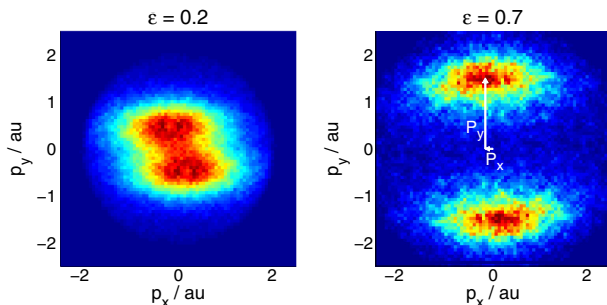


FIG. 1 (color online). Experimentally measured electron momenta distributions in the plane of laser polarization at lower ($\epsilon = 0.2$) and higher ($\epsilon = 0.7$) values of ellipticity. The coordinates of the center are labeled in the right panel with P_x and P_y .

after strong field ionization of helium over a complete scan of ellipticity ϵ of the laser field. The details of the experiment are given elsewhere [5]. In summary, the experimental setup used COLTRIMS [28] with a laser pulse duration (full width at half maximum) of 33 fs, peak intensity of $8 \times 10^{14} \text{ W cm}^{-2}$, and central wavelength of 788 nm. An ellipticity scan was performed using a broadband quarter-wave plate, which was rotated continuously. The electron momenta at the detector were recorded for different values of ϵ , ranging from linearly to near-circularly polarized light. The ellipticity scan corresponded to the range of the Keldysh parameter $\gamma = 0.5\text{--}0.7$, where γ is given by $\gamma = \omega\sqrt{2I_p(\epsilon^2 + 1)}/F_0$, and $\gamma < 1$ is considered the tunneling regime [8,29]. We were, therefore, able to investigate the impact of the force of the parent ion on the tunneled electron for all laser polarizations, from linear to circular. To extract the center of the electron momenta distribution, elliptical integration was used [30]. This method is robust for all values of ellipticity, resulting in a well-defined Gaussian fit [30], without an asymmetric double-peak structure, which occurs with radial integration at low ϵ [5,11].

We find that while the force exerted by the parent ion along the minor axis of polarization is negligible at higher ellipticities of laser light, it can be significant at lower values of ϵ . These experimental results are shown in Fig. 2, where the location of the center of the electron momenta distribution along the minor axis of polarization P_y is compared with the analytical prediction, given by Eq. (2). As can be seen from Fig. 2, neglecting the Coulomb force on electron momentum along the minor axis of polarization, or the y axis, results in excellent agreement between theory and experiment for $\epsilon \geq 0.3$. For smaller values of ϵ , the change in momentum due to the interaction of the electron with the parent ion is substantial. This results in significant Coulomb focusing along the minor axis of polarization,

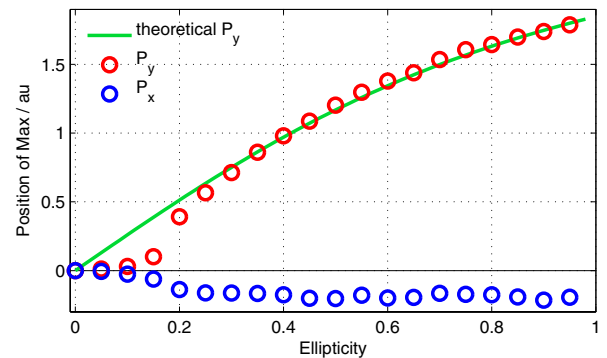


FIG. 2 (color online). Center of the electron momenta distributions P_x and P_y along the major and minor axis of polarization, respectively, obtained from experiment. Theoretical curves correspond to expected values in the absence of any Coulomb interaction for P_y (green curve) and P_x (horizontal black line).

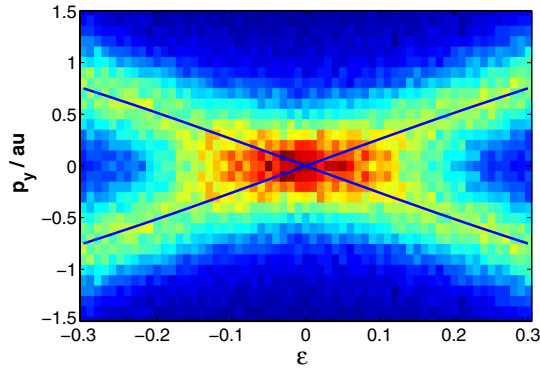


FIG. 3 (color online). Experimentally measured electron momenta distributions along the minor axis of polarization as a function of ellipticity. The blue line is given by Eq. (2). A bifurcation occurs near $\epsilon \approx \pm 0.1$.

shown in Fig. 3, which plots electron momenta distributions along the y axis as a function of ϵ . From Fig. 3, it is clear that a bifurcation occurs around the absolute value of $\epsilon \approx 0.1$, leading to the splitting of the electron momenta distribution and the loss of Coulomb focusing.

To calculate this bifurcation value, we use the condition $P_y + \Delta P_y \approx 0$, with P_y given by Eq. (2) and ΔP_y calculated by following the unperturbed trajectory $\vec{r}(t)$ of the electron in the laser field [10]:

$$\Delta \vec{P} \approx - \int_0^\infty (\vec{r}(t)/r^3(t)) dt. \quad (3)$$

The bifurcation value ϵ_b can then be obtained by solving the following equation for ϵ

$$\frac{1}{\omega} \int_0^\infty dt \frac{\omega t - f(t) \sin(\omega t)}{(x_0^2(t, \epsilon) + y_0^2(t, \epsilon))^{3/2}} = 1, \quad (4)$$

where $x_0(t, \epsilon)$ and $y_0(t, \epsilon)$ are electron trajectories in the absence of the Coulomb force, provided in Ref. [21]. Solving the above equation numerically, we obtain $|\epsilon_b| \approx 0.06$, in approximate agreement with the experimental value of $|\epsilon_b| \approx 0.1$, shown in Fig. 3. The discrepancy between the analytic and experimentally obtained estimates of ϵ_b is in part explained by considering that the location of P_y at zero for low values of ϵ is not due exclusively to the Coulomb correction, but also to the fact that a double peak is not formed immediately as two Gaussian distributions begin to separate with increasing value of ϵ . Another factor is that a perturbative approach tends to underestimate the total Coulomb correction. Overall, the analysis supports the conclusion that the bifurcation point corresponds to the value of ϵ where the Coulomb force becomes too weak to offset the velocity drift along the minor axis of polarization created by the laser field.

We next investigate the Coulomb effect on momentum following the commonly used approach first proposed

by Goreslavski *et al.* [10], finding that it fails to correctly predict both the values of P_x and P_y at low ellipticities. In particular, this method predicts a correction to P_x , and no correction to P_y . Looking at Fig. 2, it is clear that the situation is actually reversed: there is a noticeable correction to P_y (causing it to deviate from the Coulomb-free theoretical curve) and virtually no correction on P_x for $\epsilon < 0.1$.

The method in Ref. [10] assumes that the momentum correction from the parent atom can be estimated by only considering the dynamics immediately after ionization, while the electron is still close to the tunnel exit. To calculate this correction to the momentum, the electron trajectory at the peak of the laser field is approximated by [10] $\vec{r}(t) = (x_e + (1/2)F_{\max} t^2)\hat{x}$, where $F_{\max} = F_0/\sqrt{\epsilon^2 + 1}$. The Coulomb correction to the center of the electron momenta distribution is then calculated by substituting this $\vec{r}(t)$ into Eq. (3). Since the maxima of the electric field points in the x direction, the Coulomb correction causes a shift only along the x axis, predicting no change in momentum along the minor axis of polarization. Based on this calculation, there should have been complete agreement between the experimental measurements for P_y and the theoretical curve plotted in Fig. 2.

For nonzero initial transverse velocity, the Coulomb correction along y is predicted to be nonzero in Ref. [10], but is likewise negligibly small, and so does not seem to account for our experimental findings. In particular, in Ref. [12], it was found, following the approach in Ref. [10], that for $\epsilon = 0.1$, $\Delta P_y/P_y \leq 0.06$, where ΔP_y is the Coulomb correction to the momentum along the minor axis and P_y is the corresponding unperturbed momentum. Here on the contrary, our experimental results show that for $\epsilon \leq 0.1$, the correction to P_y completely cancels out the unperturbed drift velocity, or $\Delta P_y/P_y \approx 1$, as Fig. 2 shows.

On the other hand, following the approach in Ref. [10] we calculate a Coulomb correction that is in reasonably good agreement with our experimental data for $\epsilon \geq 0.3$. In particular, Eq. (3) gives $\Delta P_x \approx -(\pi/4)\sqrt{2/F_{\max}}x_e^{-3/2}$. Substituting the exit point calculated by using a quadratic approximation of the cubic solution in parabolic coordinates [30], $x_e = (I_p + \sqrt{I_p^2 - 4\beta F_{\max}})/2F_{\max}$, we obtain

$$P_x = \Delta P_x \approx - \frac{\pi F_{\max}}{(I_p + \sqrt{I_p^2 - 4\beta F_{\max}})^{3/2}}, \quad (5)$$

where $\beta = 1 - \sqrt{2I_p}/2$. Equation (5) is plotted along with experimental results in Fig. 4. This figure shows that the perturbative approach proposed in Ref. [10] significantly overestimates the magnitude of the Coulomb correction on momentum along the major axis of polarization at small ϵ , and slightly underestimates it at higher ϵ .

Figure 2 indicates how the two components of the center of the electron momenta distribution, given by P_x and P_y ,

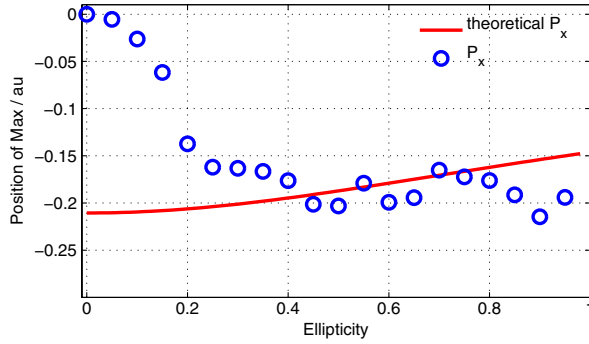


FIG. 4 (color online). Experimental values of P_x compared with the perturbative calculation, given by Eq. (5), following the approach in Ref. [10]. The Coulomb effects on P_x are negligible for $\epsilon \leq 0.1$.

can be used as complementary probes of Coulomb effects, depending on the value of ϵ . In particular, at low values of ϵ , P_x shows no evidence of Coulomb interaction, $P_x \approx 0$, while P_y shows significant deviations from theory due to Coulomb effects. This situation reverses itself as ellipticity increases. Since the deviation of P_x from zero is the underlying cause of Coulomb asymmetry [10], it serves as a sensitive probe of electron interaction with a parent ion at higher values of ellipticity, corresponding to $\epsilon \approx 0.2$ and above (see Fig. 4). On the other hand, the interaction with the parent ion leaves a significant imprint on the momentum P_y at low values of ϵ , resulting in substantial Coulomb focusing. This focusing can be seen in Fig. 3, where $P_y \approx 0$ up to the bifurcation value of around $\epsilon \approx 0.1$. This bifurcation is due to the long-range interaction with the parent ion, with blue lines in Fig. 3, given by Eq. (2), showing that no such bifurcation occurs when this interaction is absent. Hence, Coulomb focusing is a sensitive indicator of the electron-ion interaction at low ellipticities of laser light, with Coulomb asymmetry becoming significant just as Coulomb focusing begins to break down.

It is clear that the absence of Coulomb asymmetry, characterized by $P_x = 0$, means that the approach in Ref. [10], which always predicts a nonzero value of P_x [see Eq. (5) and Fig. 4], fails at low epsilon, predicting a significant asymmetry which is not actually observed. Figure 4 illustrates this, showing that Ref. [10] indeed fails for low ellipticities, but becomes quite accurate for ϵ values higher than about 0.3. To understand why, we performed classical trajectory simulations of electrons after strong field tunnel ionization, following the method described in Ref. [30]. We then extracted the trajectories with final momenta corresponding to those found at the center of the momenta distribution (CMD) measured in our experiment. The results clearly show (see Fig. 1S in Ref. [31]) that at lower values of ellipticity, the CMD trajectories are not ionized at the peak. Therefore, the failure of Ref. [10] at lower ellipticities seems to be, at least partly, due to the fact that the trajectories with the highest probability of tunneling do not find

their way to the CMD. Given that Rydberg capture and rescattering can be quite significant at lower ellipticities, but almost completely disappears for $\epsilon > 0.3$, as was found in Refs. [32,33], it seems plausible that many of the same tunneled electron trajectories which end up in the CMD at higher ellipticities, either rescatter or are captured into Rydberg states at low values of ellipticity. This would explain why the highest density of trajectories at low ellipticities seems to come before the peak, where the probability of ionization is not the highest. This explanation is supported by a prior experiment [33] that shows that the percentage of electrons captured into Rydberg states via the process of frustrated tunnel ionization is significant for our experimental parameters at low ellipticity: around 10 percent for linear polarization and quickly decreasing with increasing epsilon. Moreover, another work [21] derives a probability distribution of Rydberg states as a function of ellipticity, showing that a large fraction of Rydberg states formed by frustrated tunnel ionization come from ionization near the peak of the laser field, thereby preventing the observation of these electrons at the detector.

In conclusion, our study offers a unified approach to direct experimental investigation of the role of long-range potentials in strong field laser-atom interaction. We use the center of the electron momenta distribution, which is both experimentally easy to access and robust to noise. Our conclusions do not rely on classical trajectory simulations or on momenta spreads (which, while experimentally accessible, are more affected by uncertainties, such as thermal ion spreads if COLTRIMS is used [5,13]). We observe significant long-range electron-ion interaction along the minor axis of polarization at low ellipticities of laser light, leading to substantial Coulomb focusing and bifurcation in the electron momentum. Our results complement prior studies that found significant Coulomb focusing perpendicular to the polarization plane for low ellipticities of laser light [13,34]. Since Coulomb interaction along the minor axis of polarization is normally neglected in the analysis of electron dynamics [6,11,12], and does not appear in standard calculations of the Coulomb effects [10], an alternative calculation is presented that shows approximate agreement with the experimental bifurcation value.

The breakdown of Coulomb focusing and the onset of Coulomb asymmetry are shown to occur around the same value of ellipticity of laser light. Both effects are caused by the departure of the center of the electron momenta distribution from zero and, hence, to a substantial decrease of zero energy states, and, consequently, Rydberg states [21]. Our results point to a common underlying mechanism behind the breakdown of Coulomb focusing, the onset of Coulomb asymmetry, and the loss of Rydberg electrons with increasing ellipticity of laser light.

This work was supported by the NCCR Molecular Ultrafast Science and Technology (NCCR MUST) program, funded by the Swiss National Science Foundation (SNSF),

by ETH Research Grant No. ETH-03 09-2, and by a SNSF equipment grant. Our ultrafast activities are supported by the ETH Femtosecond and Attosecond Science and Technology (ETH-FAST) initiative as part of the NCCR MUST program. A. S. L. is supported by the FP7 IIF Grant No. 275313.

*alexandra.landsman@phys.ethz.ch

- [1] M. Uiberacker *et al.*, *Nature (London)* **446**, 627 (2007).
- [2] P. Eckle, A. N. Pfeiffer, C. Cirelli, A. Staudte, R. Dörner, H. G. Muller, M. Büttiker, and U. Keller, *Science* **322**, 1525 (2008).
- [3] A. N. Pfeiffer, C. Cirelli, M. Smolarski, D. Dimitrovski, M. Abu-samaha, L. B. Madsen, and U. Keller, *Nat. Phys.* **8**, 76 (2012).
- [4] A. D. Bandrauk and S. Chelkowski, *Phys. Rev. Lett.* **84**, 3562 (2000).
- [5] A. N. Pfeiffer, C. Cirelli, A. S. Landsman, M. Smolarski, D. Dimitrovski, L. Madsen, and U. Keller, *Phys. Rev. Lett.* **109**, 083002 (2012).
- [6] D. Shafir, H. Soifer, B. D. Bruner, M. Dagan, Y. Mairesse, S. Patchkovskii, M. Yu. Ivanov, O. Smirnova, and N. Dudovich, *Nature (London)* **485**, 343 (2012).
- [7] F. Krausz and M. Ivanov, *Rev. Mod. Phys.* **81**, 163 (2009).
- [8] L. V. Keldysh, *JETP* **20**, 1307 (1965).
- [9] H. R. Reiss, *Phys. Rev. A* **22**, 1786 (1980).
- [10] S.P. Goreslavski, G. Paulus, S. Popruzhenko, and N. Shvetsov-Shilovski, *Phys. Rev. Lett.* **93**, 233002 (2004).
- [11] M. Li, Y. Liu, H. Liu, Q. Ning, L. Fu, J. Liu, Y. Deng, C. Wu, L. Peng, and Q. Gong, *Phys. Rev. Lett.* **111**, 023006 (2013).
- [12] N. Dudovich, J. Levesque, O. Smirnova, D. Zeidler, D. Comtois, M. Ivanov, D. Villeneuve, and P. Corkum, *Phys. Rev. Lett.* **97**, 253903 (2006).
- [13] D. Shafir, H. Soifer, C. Vozzi, A. S. Johnson, A. Hartung, Z. Dube, D. M. Villeneuve, P. B. Corkum, N. Dudovich, and A. Staudte, *Phys. Rev. Lett.* **111**, 023005 (2013).
- [14] R. Landauer and Th. Martin, *Rev. Mod. Phys.* **66**, 217 (1994).
- [15] G. L. Yudin and M. Y. Ivanov, *Phys. Rev. A* **63**, 033404 (2001).
- [16] T. Brabec, M. Y. Ivanov, and P. B. Corkum, *Phys. Rev. A* **54**, R2551 (1996).
- [17] P. B. Corkum, *Phys. Rev. Lett.* **71**, 1994 (1993).
- [18] T. F. Gallagher, *Phys. Rev. Lett.* **61**, 2304 (1988).
- [19] H. B. van Linden van den Heuvell and H. G. Muller, in *Multiphoton Processes*, edited by S. J. Smith and P. L. Knight (Cambridge University Press, Cambridge, England, 1988).
- [20] K. C. Kulander, K. J. Schafer, and J. L. Kause, in *Super-Intense Laser-Atom Physics*, edited by B. Piraux, A. L'Huillier, and K. Rzazewski (Plenum, New York, 1993), p. 95.
- [21] A. S. Landsman, A. N. Pfeiffer, C. Hofmann, M. Smolarski, C. Cirelli, and U. Keller, *New J. Phys.* **15**, 013001 (2013).
- [22] B. Bergues *et al.*, *Nat. Commun.* **3**, 813 (2012).
- [23] A. S. Landsman, S. A. Cohen, and A. H. Glasser, *Phys. Rev. Lett.* **96**, 015002 (2006).
- [24] A. S. Landsman, S. A. Cohen, and A. H. Glasser, *Phys. Plasmas* **11**, 947 (2004).
- [25] S. A. Cohen, A. S. Landsman, and A. H. Glasser, *Phys. Plasmas* **14**, 072508 (2007).
- [26] M. V. Ammosov, N. B. Delone, and V. P. Krainov, *Sov. Phys. JETP* **64**, 199 (1986).
- [27] R. Boge, C. Cirelli, A. S. Landsman, S. Heuser, A. Ludwig, J. Maurer, M. Weger, L. Gallmann, and U. Keller, *Phys. Rev. Lett.* **111**, 103003 (2013).
- [28] R. Dörner, V. Mergel, O. Jagutzki, L. Spielberger, J. Ullrich, R. Moshhammer, and H. Schmidt-Böcking, *Phys. Rep.* **330**, 95, (2000).
- [29] C. H. Raymond Ooi, W. L. Ho, and A. D. Bandrauk, *Phys. Rev. A* **86**, 023410 (2012).
- [30] C. Hofmann, A. S. Landsman, C. Cirelli, A. N. Pfeiffer, and U. Keller, *J. Phys. B* **46**, 125601 (2013).
- [31] See Supplemental Material at <http://link.aps.org/supplemental/10.1103/PhysRevLett.111.263001> for simulations showing the phase of ionization for electrons found at the center of the momenta distribution at the detector.
- [32] A. S. Landsman, A. N. Pfeiffer, M. Smolarski, C. Cirelli, and U. Keller, *Eur. Phys. J. Web Conf.* **41**, 02018 (2013).
- [33] T. Nubbemeyer, K. Gorling, A. Saenz, U. Eichmann, and W. Sandner, *Phys. Rev. Lett.* **101**, 233001 (2008).
- [34] D. Comtois, D. Zeidler, H. Pépin, J. C. Kieffer, D. M. Villeneuve, and P. B. Corkum, *J. Phys. B* **38**, 1923 (2005).